Advanced Active Imaging with Single Photon Avalanche Diodes

Martin Laurenzis[a], Marco La Manna[b], Mauro Buttafava[c], Alberto Tosi[c], Ji-Hyun Nam[b], Mohit Gupta[d], and Andreas Velten[b]

[a]Advanced Vision and Processing, French-German Research Institute of Saint-Louis, Saint-Louis, France
[b]Computational Optics Group, University of Wisconsin-Madison, Madison (WI), USA
[c]Dipartimento di Elettronica, Informazione e Bioingegneria, Politecnico di Milano, Milan, Italy
[d]Department of Computer Science, University of Wisconsin-Madison, Madison (WI), USA

ABSTRACT

Ranging and imaging in low light level conditions are a key application of active imaging systems. Typically, intensified cameras (ICCD, EBCMOS) are used to sense the intensity of reflected laser light pulses used for illumination. Recent developments in single photon avalanche diodes (SPAD) show, that sensors having single photon counting capabilities are about to revolutionize low light level imaging and laser ranging. These sensors have the ability to count detection events caused by single photons with very high timing precision. By application of statistical measurement means, the sensitivity of such devices can be increased far beyond classical sensing devices and the needed photon flux has significant lower intensities. New SPAD devices enable the development of novel sensing methods and technologies, and open laser ranging and imaging to new fields of application. Here, we focus on novel hardware structures which are under development as well as the application of avalanche photo diode detectors for light-in-flight detection and non-line-of-sight imaging.

Keywords: Compressed range imaging, ranging, LiDAR, LADAR

1. INTRODUCTION

Active imaging systems such as Laser Gated Viewing[1,2] as well as scanning[3,4] and flash imaging LiDAR[2] are widely used in civilian (e.g. automotive and autonomous driving) and military remote sensing operations for surveillance and situational awareness tasks. Both imaging and/or ranging capabilities are requested in various scenarios like navigation in high dynamics and complex scenes (e.g. autmotive), vision at low light level (i.e. night vision) or hash weather conditions (e.g. maritime or submarine environments) are key application of active imaging systems. Due to the demand of either fast data acquisition and/or low number of usable returning photons, intensified sensor systems like intensified cameras (ICCD, EBCMOS) or avalanche photo diodes (APD) are used to sense the transient intensity of reflected laser light pulses used for illumination or to temporally filter out usable information by fast gating.

Recent developments in Single-Photon Avalanche Diodes (SPADs)[5–10] show that sensors having single photon counting capabilities are about to revolutionize low light level imaging and laser ranging. These sensors have the ability to count detection events caused by single photons with very high timing precision. Exploiting statistical measurements,[11,12] the sensitivity of such devices can be increased far beyond classical sensing devices and the needed photon flux has significant lower intensities. New SPAD devices enable the development of novel sensing methods and technologies, and open laser ranging and imaging to new fields of application. Here, we focus on novel hardware structures which are under development as well as the application of avalanche photo diode detectors for light-in-flight detection and non-line-of-sight imaging.

Further author information: (Send correspondence to M.L.)
M.L.: E-mail: martin.laurenzis@isl.eu, Telephone: +33 3 89 69 1000

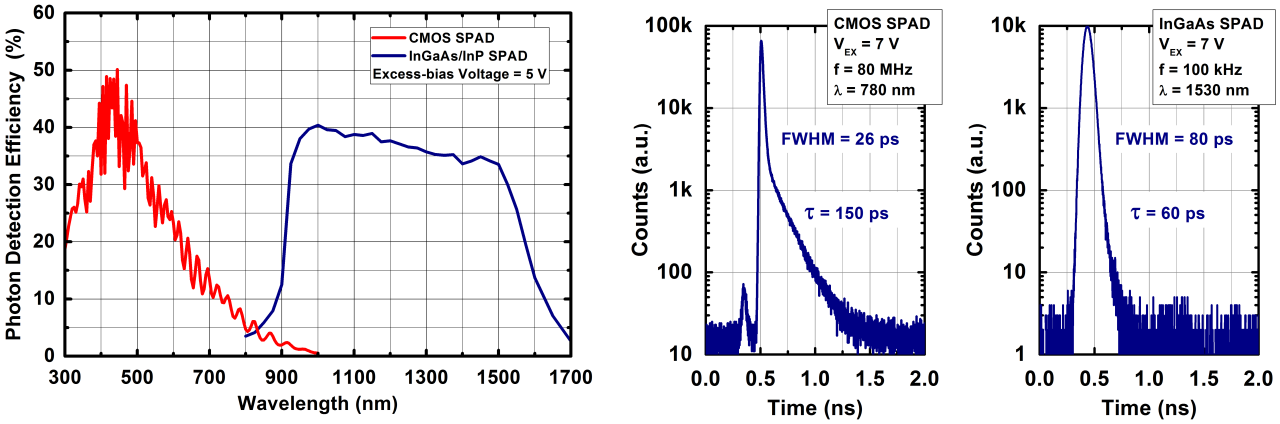

(a) (b) (c)

Figure 1. Typical Photon Detection Efficiency (PDE) curve of silicon and InGaAs/InP SPADs (a). Impulse response function to a narrow laser pulse for both silicon (b) and InGaAs/InP (c) SPADs, acquired using the TCSPC technique.

2. SINGLE-PHOTON AVALANCHE DIODE TECHNOLOGY

The SPAD is a solid-state single-photon detector capable of measuring extremely fast and weak light signals. The detector is basically a p-n junction that is reverse biased above the breakdown voltage (by an amount called excess bias), in which the electric field within the active area is sufficiently high to allow the triggering of a self-sustaining impact ionization process (avalanche), even starting from a single photo-generated charge carrier.[5] The result is a macroscopic current pulse, whose leading edge marks the arrival time of the absorbed photon, with tens of picoseconds precision.

Silicon SPADs can cover the wavelength range from 300 nm to 900 nm, exhibiting a Photon Detection Efficiency (PDE) greater than 45% at 500 nm and few percent at 900 nm (cf. Figure 1 (a), red curve). Note that the carrier thermal generation can also trigger an avalanche pulse without any absorbed photon and this effect is quantified by the Dark Count Rate (DCR). The DCR is the main noise contribution in a SPAD detector and for a typical silicon CMOS device, having an active area diameter of 50 μm, it is in the order of few tens of counts/s at 300 K, decreasing with temperature and with excess bias voltage.[5–7] A typical silicon SPAD impulse response function, shown in Figure 1 (b), is composed by two contributions: a main peak and an exponential tail.[5] Photons absorbed into the depleted region trigger a fast avalanche ignition, with a time-jitter due to the statistical fluctuation of the avalanche buildup, and give rise to the main peak. Photons absorbed in the neutral region (either below or above the depleted one) generate carriers that slowly diffuse and, in some cases, reach the depleted region originating the slower tail. The Full-Width at Half Maximum (FWHM) of the main peak is the intrinsic time resolution of the detector, which can reach values lower than 30 ps in systems currently used for Non-Line Of Sight (NLOS) imaging.[13]

The InGaAs/InP SPAD is currently the best choice for extending the sensitivity to the near-infrared wavelength range between 900 nm and 1700 nm, with a PDE higher than 40%[8,14] (cf. Figure 1 (a), blue curve). Such InGaAs/InP SPAD detectors with a 25 μm active-area diameter have a DCR of few kcounts/s at 225 K (temperature that can be easily achieved with compact 3-stage thermo-electric cooler).[14] Furthermore, their temporal response can be narrower than 80 ps FWHM and almost free from any slow diffusion tail after the main peak, as shown in Figure 1 (c).

An important advantage of a SPAD detector in time-of-flight imaging applications is the possibility of turning it ON and OFF quickly and efficiently, modulating its bias voltage from below to above the breakdown level. A photon impinging on the detector during its OFF time is not able to trigger any avalanche. A gated-mode operated SPAD with transition times between OFF and ON conditions shorter than 1 ns is known in literature as a fast-gated SPAD. This operating mode is very useful to perform a time filtering of incoming photons, for example in NLOS imaging applications. In these cases, it is extremely important to reject the strong light pulse

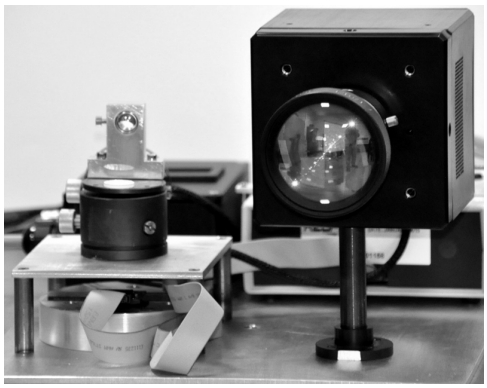

Figure 2. Laboratory setup of a Geiger-mode avalanche photo diode camera and a fiber laser illumination device.

from the first reflection on the relay wall, in order to avoid the loss of useful later photons arriving when the SPAD and/or timing electronics are within their dead-times. After each photon detection, the SPAD has to be kept OFF for a certain amount of time (hold-off time) in order to reduce the afterpulsing effect probability.[5] Typical hold-off times are in the order of tens of nanoseconds for silicon SPADs and few microseconds for InGaAs/InP ones, while timing electronics (i.e. Time-Correlated Single-Photon Counting -TCSPC- instruments) exhibit a conversion time in the order of 100 ns.[15,16]

Photon counting systems based on single-pixel fast-gated SPADs are currently employed in NLOS imaging, along with a laser scanner to cover the relay wall surface.[17] However, a single-point detection has the drawback of a limited acquisition speed (tens of seconds or higher), preventing the capability of tracking moving objects. Time-of flight imaging using 2D SPAD arrays can overcome this important limitation and it has been demonstrated in various applications,[9,18] but with no fast-gating capability. Recently a very compact custom integrated circuit for SPAD fast-gating has been demonstrated, capable to operate both silicon and InGaAs/InP SPADs with transition times below 300 ps and temporal resolution below 50 ps FWHM.[19] Thanks to these achievements, the integration of fast-gating electronics together with Time-to-Digital Converters (TDCs) into the same CMOS SPAD chip will be the starting point for the development of 2D fast-gated SPAD arrays tailored for NLOS imaging.

3. ADVANCED SENSING CAPABILITIES

Both the enormous high sensibility and the capability of high resolution transient recording enable new application fields for active imaging systems based on single-photon avalanche detectors. In the following section, we focus on two exemplary novel sensing approaches which illustrates the dawn of a new sensor generation: Light-in-Flight imaging and Non-Line-of-Sight sensing.

3.1 Visualize and trace back Light-in-Flight

In the past, observation of light-in-flight was only possible by indirect means (i.e. interaction with a holographic medium[20] or reflection from strong reflecting or scattering medium or interface). Thanks to recent improvements in sensor development, state of the art single photon counting array devices are capable to sense sparsely scattering signatures from laser pulses propagating through and scattered by air.[18,21–23] Using a single photon counting camera, consisting of a low dark current SPAD array detector, and a high resolution transient recorder device for each sensor element, it is possible to sense the trace of very low light signatures.

We depict in Figure 2 the setup used in the following experiment. Specifically, the setup consists of a Geiger-mode InGaAs avalanche photo diode camera with an array size of 32×32 sensor elements and a Erbium-doped fiber laser. Each sensor element can measure the temporal occurrence of an event, namely the single photon time-of-flight within a timing window of 8000 time bins with a resolution of 250 ps at a maximum frame rate of 80 kHz. The laser source emits pulses at 1.545 nm with a pulse width of 500 ps and a repetition rate of 50 kHz. The overall system is able to measure the photon time-of-flight in over 1000 sensor elements with a frame rate of 50 kHz and an accuracy of about 700 ps.

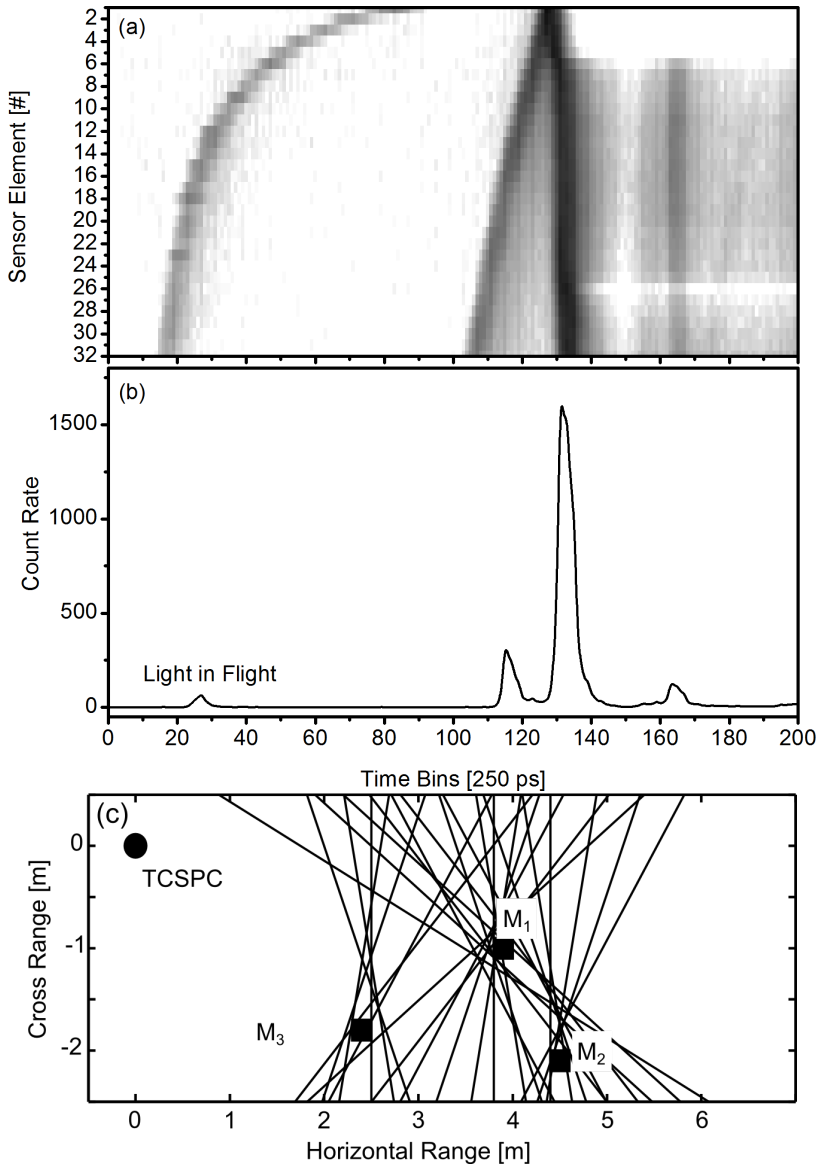

Figure 3. Light-in-Flight imaging: transient sensor data for a sensor line (a) and a single sensor (b), (c) tracing back laser light to its origin.

In Figure 3 (a) and (b), single photon counting data are depicted for a sensor line (32 detectors) and a single element, respectively. The data represents histograms of multiple measurement frames. As a first signature, a laser pulse is propagating from the right to the left through the sensor's field of view, leaving a trace between 18 ns and 90 ns. Later, multiple reflections from a wall in the sensor's field of view can be observed. These signatures arise from direct illumination of the wall or indirect illumination with multi-bounce photons.

It can be shown[22,23] that the bending of the laser pulse trace contains sufficient information to reconstruct the propagation path, even if the single photon counting camera is not precisely synchronized to the laser pulse emission.[23] The curving or bending of the signature can be analyzed determining the time difference of arrival for different reception angles and its comparison to theoretical values, defined as

$$TDOA_{i,j} = \frac{\overline{P_iP_j} + \overline{P_jS} - \overline{P_iS}}{c} = \frac{d}{c}\frac{\sin\alpha}{\sin(\alpha+\theta_i)}\left(\frac{\sin(\theta_i+\theta_j)-\sin(\alpha-\theta_j)}{\sin(\alpha-\theta_j)} - 1\right) \quad (1)$$

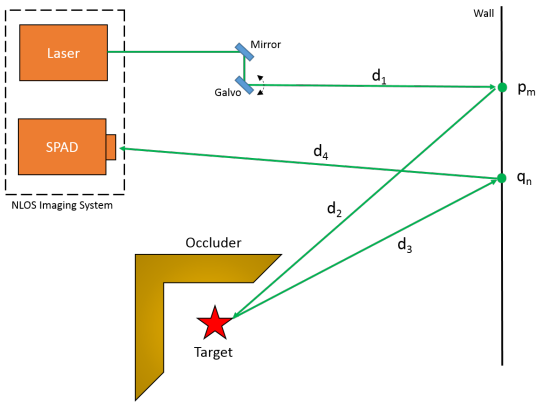

Figure 4. An example of optical NLOS scenario, where a target is not in the direct line-of-sight of the imaging system and hidden by an occluder. The goal of the reconstruction algorithm is to exploit the time information embedded in the scattered photons to recover the 3D image of the target.

By analyzing different points (P_i, P_j) of the trajectory, a model can be derived to determine the propagation path of the laser light using the observation angle $(\theta_{i,j})$ relative to the optical axis of the sensor device. The propagation path is determined by two values: the range or distance from the sensor system (d) and the propagation angle (α) relative to its optical axis.

In Figure 3 (c), exemplary results are presented showing the analysis of a series of datasets. The data was recorded for light pulses which were deflected by a mirror placed at three different positions, M_1, M_2 and M_3 (rotating the mirror causes the laser to propagate at different angles). In the analysis, the time difference of arrival from a set of three points (entrance, middle and exit point) are analyzed for each trajectory. The reconstructed traces concentrate around the locations M_1, M_2 and M_3, where mirrors are placed during the measurements. Unfortunately, the reconstruction accuracy is limited due to the limited temporal resolution of the setup ($\approx$ 700 ps). Details of this measurement can be found in the literature.[22,23]

3.2 Non-line-of-sight

In Figure 4, we depict a typical optical NLOS scenario, which comprises an optical imaging system, such as a light source and a camera (i.e.: SPAD), and a hidden volume (including the target), $\boldsymbol{V}$ that we wish to reconstruct. The goal is to collect photons that have scattered multiple times in the hidden volume and use their time-of-flight information to reconstruct the 3D image of the target, as well as for tracking purposes.[17,24–36]

For the remainder of the discussion, we assume that the surfaces in the considered scenario are Lambertian, namely the photons arriving at these surfaces are uniformly scattered in all directions.

Let the light source be a laser unit capable of emitting femto or picosecond long pulses at a given pulse repetition rate and let it also be collimated on a point p_m of the relay wall, whose distance w.r.t. the laser origin is d_1. Furthermore, we assume that the SPAD is focused on a wall point q_n and its distance from this point is d_4.

Once the photons arrive at the wall, they scatter in all directions (since the surface is Lambertian) and fraction of these reaches the target, traveling a distance d_2. Assuming no target inter-reflection and no sub-surface scattering, part of the photons that arrived at the target travel back to the wall, after traveling a distance d_3. In particular, the ones reaching q_n are going to be collected by the sensor. The acquired data is a function of the laser position on the wall, the SPAD focus position on the wall and time and it can be then expressed as

$$\boldsymbol{s}(p_n, q_m, t) = \mathcal{F}(\boldsymbol{b}), \tag{2}$$

where $\boldsymbol{s}$ is the acquired dataset and $\boldsymbol{b}$ is the scene's albedo (or intensity). Furthermore, $\mathcal{F}(\cdot)$ corresponds to the light transport function, which describes how the photons travel in the scene; $\mathcal{F}(\cdot)$ is scene-dependent and is

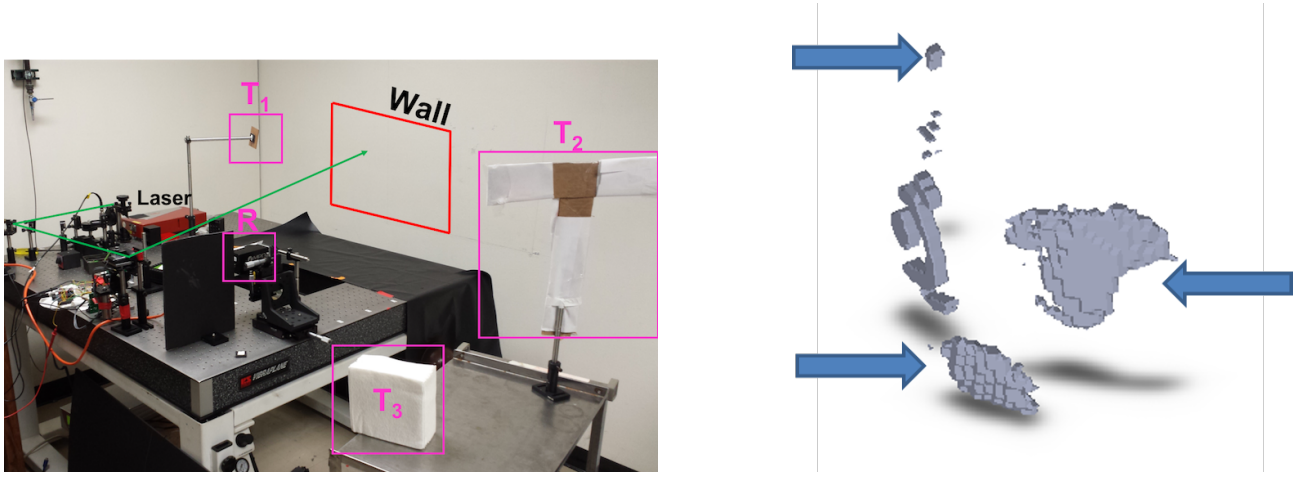

(a) (b)

Figure 5. The experimental scenario used in[17] and shown in (a) comprises a NLOS imaging system and three different targets (T_1, T_2 and T_3) placed at different location inside a volume hidden from the laser and SPAD. The reconstructed volume using the back-projection algorithm is shown in (b) and it was obtained using UCSF's Chimera rendering software.[47]

a well studied problem in the computer vision community.[37–42] Having fixed the laser and SPAD wall position (p_m and q_n, respectively), (2) essentially represents the number of photons arriving at the SPAD as a function of time.

The NLOS imaging reconstruction is the inverse problem of (2): given the acquired data $\boldsymbol{s}$, the goal is to recover $\boldsymbol{b}$, the albedo of the scene under investigation. Previous publications[17,26,27,30,43] have shown a reconstruction algorithm that is based on the backprojection method, widely employed in CT imaging.[44] In a nutshell, the reconstruction algorithm discretizes the hidden volume into unit-cube sized voxels, $v_k \in \boldsymbol{V}$, with a given side length and, for each v_k, finds its b_k. The photon count stored in $\boldsymbol{s}$ is projected to a 3D ellipsoid inside the volume, whose foci are the laser and SPAD position on the wall, p_m and q_n, respectively.

In Figure 5, we show the experimental scenario and subsequent 3D reconstruction results of the NLOS imaging system. Specifically, the system is composed of a 50 mW, 532 nm light source with a pulse duration of 250 fs and a repetition rate of 55 MHz. The sensor is an MPD's silicon gated SPAD,[13] indicated as R in Figure 5a, with a 20 μm active area, focused on a 1 cm^2 wall area. The targets comprise a white, small square patch (T_1 in Figure 5a), a white, 38 $\times$ 40 cm letter T (T_2 in Figure 5a) and a big, white square patch (T_3 in Figure 5a). All of them are not in the direct path of either the laser or the SPAD. The dataset was acquired using 185 laser positions and a single SPAD position. In Figure 5b, we show the reconstructed 3D volume, which encompasses all three targets. It is possible to see that all the targets were recovered correctly.

It is worth noting that, under certain conditions (such as absence of multi-bounce and occlusions), the problem defined in (2) can be linearized and its inverse can be solved using convex optimization-based algorithms together with fine tuned regularizers, using data acquired with off-the-shelf light sources and cameras.[28,29,45,46] Although these methods are valid alternative solutions, they come with some limitations; specifically, they can be employed to recover the 3D image of small volumes, since the matrix representing the linearized light transport function may become too big to be stored on hardware (its size is a function of the number of laser positions, SPAD positions on the wall, time and size of the scene). Furthermore, the recovery algorithms work relatively well for simple scenes, such as regular letter-shaped targets painted with retro-reflective material[46] on a completely black background and fairly close to the relay wall.

4. DISCUSSION AND CONCLUSION

In this paper, we have shown latest development in optical sensor development which are capable to detect single photons and measure their time-of-flight. State of the art SPAD sensors have an intrinsic time resolution better

than 100 ps (e.g. Si-SPAD: 26 ps, InGaAs-SPAD: 80 ps) and fast gating capabilities. Currently, these sensors are revolutionizing the field of low light level optical sensing and offer new opportunities for system layout and novel sensing approaches. Here, we demonstrated two approaches: Light-in-flight imaging and non-line-of-sight sensing.

The high sensitivity of these new sensors enable the direct observation of light pulses while propagating through air. The low intensity signal is generated by sparse scattering. It is possible to trace back light pulses to their origin even if the sensing system is not perfectly synchronized to the laser emission.

In recent years, non-line-of-sight sensing has been established to extent the optical sensor perception area to locate reflecting surfaces which are located outside the sensor's field-of-view or direct line-of-sight. This non-imaging data acquisition needs single photon detection devices with high resolution transient sensing and strong analysis algorithms to perform a high resolution back-projection of the recorded transient data. The position and shape of objects with homogeneous texture can be reconstructed with relatively high accuracy.

In conclusion, the enormous improvements in single photon counting sensor development enable the realization of novel sensing approaches which can bring new sensing capabilities.

Acknowledgments

The authors want to acknowledge funding within the REVEAL (Revolutionary Enhancement of Visibility by Exploiting Active Light-fields) program by the Defense Sciences Office of the Defense Advanced Research Projects Agency (DARPA), Arlington, USA, through contract number HR0011-16-C-0025.

REFERENCES

[1] Gillespie, L. F., "Apparent illuminance as a function of range in gated, laser night-viewing systems," *JOSA* **56**(7), 883–887 (1966).

[2] McManamon, P. F., "Review of ladar: a historic, yet emerging, sensor technology with rich phenomenology," *Optical Engineering* **51**(6), 060901 (2012).

[3] Buller, G. and Wallace, A., "Ranging and three-dimensional imaging using time-correlated single-photon counting and point-by-point acquisition," *IEEE Journal of Selected Topics in Quantum Electronics* **13**(4), 1006–1015 (2007).

[4] McCarthy, A., Krichel, N. J., Gemmell, N. R., Ren, X., Tanner, M. G., Dorenbos, S. N., Zwiller, V., Hadfield, R. H., and Buller, G. S., "Kilometer-range, high resolution depth imaging via 1560 nm wavelength single-photon detection," *Optics Express* **21**(7), 8904–8915 (2013).

[5] Zappa, F., Tisa, S., Tosi, A., and Cova, S., "Principles and features of single-photon avalanche diode arrays," *Sensors and Actuators A: Physical* **140**(1), 103–112 (2007).

[6] Ghioni, M., Gulinatti, A., Rech, I., Zappa, F., and Cova, S., "Progress in silicon single-photon avalanche diodes," *Journal of Selected Topics in Quantum Electronics* **13**(4), 852–862 (2007).

[7] Villa, F., Bronzi, D., Zou, Y., Scarcella, C., Boso, G., Tisa, S., Tosi, A., Zappa, F., Durini, D., Weyers, S., Paschen, U., and Brockherde, W., "CMOS SPADs with up to 500 μm diameter and 55% detection efficiency at 420 nm," *Journal of Modern Optics* **61**(2), 102–115 (2014).

[8] Entwistle, M., Itzler, M. A., Chen, J., Owens, M., Patel, K., Jiang, X., Slomkowski, K., and Rangwala, S., "Geiger-mode apd camera system for single photon 3-d ladar imaging," in [*Advanced Photon Counting Techniques VI*], *Proc. of SPIE* **8375**, 83750D, SPIE (2012).

[9] Shin, D., Xu, F., Venkatraman, D., Lussana, R., Villa, F., Zappa, F., Goyal, V. K., Wong, F. N., and Shapiro, J. H., "Photon-efficient imaging with a single-photon camera," *Nature Communications* **7**, 12046 (2016).

[10] Zhang, J., Itzler, M. A., Zbinden, H., and Pan, J.-W., "Advances in ingaas/inp single-photon detector systems for quantum communication," *Light: Science & Applications* **4**(5), e286 (2015).

[11] Pawlikowska, A. M., Halimi, A., Lamb, R. A., and Buller, G. S., "Single-photon three-dimensional imaging at up to 10 kilometers range," *Optics Express* **25**(10), 11919–11931 (2017).

[12] Tobin, R., Halimi, A., McCarthy, A., Laurenzis, M., Christnacher, F., and Buller, G. S., "Depth imaging through obscurants using time-correlated single-photon counting," in [*Advanced Photon Counting Techniques XII*], **10659**, 106590S, International Society for Optics and Photonics (2018).

[13] Buttafava, M., Boso, G., Ruggeri, A., Mora, A. D., and Tosi, A., "Time-gated single-photon detection module with 110 ps transition time and up to 80 MHz repetition rate," *Review of Scientific Instruments* **85**(8), 083114 (2014).

[14] Tosi, A., Calandri, N., and Acerbi, M. S. F., "Low-noise, low-jitter, high detection efficiency ingaas/inp single-photon avalanche diode," *Journal of Selected Topics in Quantum Electronics* **20**(6), 192–197 (2014).

[15] Becker, W., ed., [*Advanced Time-Correlated Single Photon Counting Applications*], Springer International Publishing (2015).

[16] Markovic, B., Tisa, S., Villa, F., Tosi, A., and Zappa, F., "A high-linearity, 17 ps precision time-to-digital converter based on a single-stage vernier delay loop fine interpolation," *IEEE Transactions on Circuits and Systems* **60**(3), 557–569 (2013).

[17] Buttafava, M. et al., "Non-line-of-sight imaging using a time-gated single photon avalanche diode," *Optics Express* **23**, 20997–21011 (Aug 2015).

[18] Gariepy, G., Krstajić, N., Henderson, R., Li, C., Thomson, R. R., Buller, G. S., Heshmat, B., Raskar, R., Leach, J., and Faccio, D., "Single-photon sensitive light-in-fight imaging," *Nature Communications* **6**, 6021 (2015).

[19] Ruggeri, A., Ciccarella, P., Villa, F., Zappa, F., and Tosi, A., "Integrated circuit for subnanosecond gating of ingaas/inp spad," *Journal of Selected Topics in Quantum Electronics* **51**(7), 1–7 (2015).

[20] Abramson, N. H. and Spears, K. G., "Single pulse light-in-flight recording by holography," *Applied Optics* **28**(10), 1834–1841 (1989).

[21] Laurenzis, M., Klein, J., Bacher, E., and Metzger, N., "Multiple-return single-photon counting of light in flight and sensing of non-line-of-sight objects at shortwave infrared wavelengths," *Optics Letters* **40**(20), 4815–4818 (2015).

[22] Laurenzis, M., Klein, J., and Bacher, E., "Relativistic effects in imaging of light in flight with arbitrary paths," *Optics Letters* **41**(9), 2001–2004 (2016).

[23] Laurenzis, M., Klein, J., Bacher, E., Metzger, N., and Christnacher, F., "Sensing and reconstruction of arbitrary light-in-flight paths by a relativistic imaging approach," in [*Electro-Optical Remote Sensing X*], **9988**, 998804, International Society for Optics and Photonics (2016).

[24] Kirmani, A. et al., "Looking around the corner using ultrafast transient imaging," *Int. J. Comput. Vision* **95**(1), 13–28 (2011).

[25] Steinvall, O., Elmqvist, M., and Larsson, H., "See around the corner using active imaging," in [*SPIE Security and Defence*], 818605–818605, International Society for Optics and Photonics (2011).

[26] Velten, A. et al., "Recovering three-dimensional shape around a corner using ultrafast time-of-flight imaging," *Nature Communications* **3**, 745 (03 2012).

[27] Gupta, O. et al., "Reconstruction of hidden 3D shapes using diffuse reflections," *Optics Express* **20**, 19096–19108 (Aug 2012).

[28] Heide, F., Hullin, M. B., Gregson, J., and Heidrich, W., "Low-budget transient imaging using photonic mixer devices," *ACM Trans. Graph.* **32**, 45:1–45:10 (July 2013).

[29] Heide, F., Xiao, L., Heidrich, W., and Hullin, M. B., "Diffuse mirrors: 3D reconstruction from diffuse indirect illumination using inexpensive time-of-flight sensors," in [*2014 IEEE Conf. Comput. Vision Pattern Recognition*], 3222–3229 (June 2014).

[30] Laurenzis, M. and Velten, A., "Nonline-of-sight laser gated viewing of scattered photons," *Optical Engineering* **53**, 53 – 53 – 7 (2014).

[31] Laurenzis, M., Klein, J., Bacher, E., and Metzger, N., "Multiple-return single-photon counting of light in flight and sensing of non-line-of-sight objects at shortwave infrared wavelengths," *Optics Letters* **40**, 4815–4818 (Oct 2015).

[32] Gariepy, G., Tonolini, F., Henderson, R., Leach, J., and Faccio, D., "Detection and tracking of moving objects hidden from view," *Nature Photonics* (2015).

[33] Kadambi, A., Zhao, H., Shi, B., and Raskar, R., "Occluded imaging with time-of-flight sensors," *ACM Trans. Graph.* **35**, 15:1–15:12 (Mar. 2016).

[34] Klein, J., Peters, C., Martín, J., Laurenzis, M., and Hullin, M. B., "Tracking objects outside the line of sight using 2d intensity images," *Scientific Reports* **6** (2016).

[35] Chan, S., Warburton, R. E., Gariepy, G., Leach, J., and Faccio, D., "Non-line-of-sight tracking of people at long range," *Optics Express* **25**, 10109–10117 (May 2017).

[36] Pediredla, A. K., Buttafava, M., Tosi, A., Cossairt, O., and Veeraraghavan, A., "Reconstructing rooms using photon echoes: A plane based model and reconstruction algorithm for looking around the corner," in [*2017 IEEE International Conference on Computational Photography (ICCP)*], 1–12 (May 2017).

[37] Kajiya, J. T., "The rendering equation," in [*Proceedings of the 13th Annual Conference on Computer Graphics and Interactive Techniques*], *SIGGRAPH '86*, 143–150, ACM, New York, NY, USA (1986).

[38] Nayar, S. K., Ikeuchi, K., and Kanade, T., "Shape from interreflections," *International Journal of Computer Vision* **6**(3), 173–195 (1991).

[39] Seitz, S. M., Matsushita, Y., and Kutulakos, K. N., "A theory of inverse light transport," in [*Computer Vision, 2005. ICCV 2005. Tenth IEEE International Conference on*], **2**, 1440–1447, IEEE (2005).

[40] Wu, D. et al., [*Frequency Analysis of Transient Light Transport with Applications in Bare Sensor Imaging*], 542–555, Springer Berlin Heidelberg, Berlin, Heidelberg (2012).

[41] Jarabo, A., Masia, B., Marco, J., and Gutierrez, D., "Recent advances in transient imaging: A computer graphics and vision perspective," *Visual Informatics* **1**(1), 65 – 79 (2017).

[42] Tsai, C.-Y., Kutulakos, K. N., Narasimhan, S. G., and Sankaranarayanan, A. C., "The geometry of first-returning photons for non-line-of-sight imaging," in [*IEEE Intl. Conf. Computer Vision and Pattern Recognition (CVPR)*], (2017).

[43] La Manna, M., Kine, F., Breitbach, E., Jackson, J., and Velten, A., "Error backprojection algorithhms for non-line-of-sight imaging," *IEEE Transactions on Pattern Analsysis and Machine Intelligence* (2018). DOI: 10.1109/TPAMI.2018.2843363.

[44] Kak, A. and Slaney, M., [*Principles of Computerized Tomographic Imaging*], IEEE Press (1998).

[45] Heide, F., Heidrich, W., Hullin, M., and Wetzstein, G., "Doppler time-of-flight imaging," in [*ACM SIGGRAPH 2015 Emerging Tech.*], *SIGGRAPH '15*, 9:1–9:1, ACM (2015).

[46] O'Toole, M., Lindell, D., and Wetzstein, G., "Confocal non-line-of-sight imaging based on the light-cone transform," *Nature* **555**, 338 (03 2018).

[47] Pettersen, E. et al., "UCSF Chimera – A visualization system for exploratory research and analysis," *J. Comput. Chem.* **25**, 1605–1612 (2004).